Aplanatic Zone Plate Embedded in Sapphire

Zhen-Nan Tian, Jian-Guan Hua, Feng Yu, Yan-Hao Yu, Hua Liu, Qi-Dai Chen, and Hong-Bo Sun, *Fellow, IEEE*

***Abstract*— In this letter, we report the design and fabrication of an aplanatic zone plate, whose phase distribution is described by a fourth-order non-spherical function. Its optimal coefficients are determined by an iterative calculation based on the ray tracing method. The special zone plate, with a diameter of 10 mm, can significantly reduce the spherical aberration. The focal spot diameter is 43.4 μm, which is less than that of spherical lens, i.e., 153.6 μm. In addition, the zone plate is buried inside a z-cut sapphire crystal by femtosecond laser direct writing technology. This ensures that the zone plate possesses stable optical properties in complex and harsh environments. The novel embedded zone plate has an important application in optical aberration balance system. It improves the system's integration and stabilization in a high temperature environment, especially in a refractive index changing environment.**

***Index Terms*— Femtosecond laser, spherical aberration, zone plate, micro optics element, sapphire.**

I. Introduction

IN THE past decades, micro optics, as a novel branch of optics, has developed rapidly, with the urgent need of miniaturization and integration in both military and civilian optical systems [1], [2]. A variety of micro-optical components has been proposed, which played irreplaceable roles, owing to their unique optical performance [3]–[7]. Among them, the zone plate, as an outstanding representative of micro diffractive elements, has received extensive attention. The interest, ranging from theoretical design to engineering applications, is because the plate is thin, lightweight, easy to process, and has high design freedom [8], [9]. Many methods have been proposed to process a high quality zone plate, such as diamond turning [10], ion beam etching [11] and electron beam lithography [12], which increase its precision from micron to nanometer. However, the preparation of a zone plate with high precision and large size simultaneously has yet be reported. In addition, the current roles of most micro optical components are limited to qualitative focusing and imaging [11], [13]. The main optical parameter that can be provided is only focal length. The quantitative characterization of spherical aberration, astigmatism, field curvature, distortion, and other important parameters have rarely been reported. Although the optical properties of an aspherical micro lens are definitely better than those of a spherical lens, there are few reports on the quantitative comparison between the two [14]. Last year, Timo Gissibl processed a micro ultracompact multi-lens component, and compared its modulation transfer function (MTF) and longitudinal chromatic aberration, quantitatively with those of other micro components [15]. The work has been published in Nature Photonics, which attracted wide attention, and opened the door for quantitative characterization of optical properties of micro optical components.

In this work, we fabricated a large high-precision zone plate by femtosecond laser direct writing (FsLDW) technology. The diameter of the zone plate was up to 10 mm, with a small ring width of 1.33 μm. The spherical aberration was characterized quantitatively, and was significantly less than for a same-size spherical microlens. FsLDW is a mature processing technology, which is widely used in the fabrication of micro optics [16], [17], micro mechanics, micro fluidic chips [18], and microelectronics [19], owing to its excellent performance in high-precision and three-dimensional (3D) machining [20]–[22]. The zone plate was buried below the surface of a z-cut sapphire crystal based on laser inducing refractive index change [23]. The crystal surface protects the diffraction structure unit from being destroyed, which provides stable optical properties in a variety of external environments [24]. The zone plate can be used in laser processing, information reading, and an aberration balance system because of its excellent aplanatism.

II. Theory and Experiments

Spherical aberration is an inherent aberration of a spherical lens, which results in different aperture beams converging into different positions on the optical axis. In the image plane, the image spot becomes a diffuse spot. Fig. 1 shows the effect of spherical aberration on focusing based on ray tracing method. In Fig. 1(a), parallel light is incident on a spherical lens, and converges to a spot in its rear space. The beams of different apertures are represented by different color lines. The spherical lens is a plane-convex fused silica lens, whose effective optical aperture, height and curvature radius are 10 mm, 3.4 mm and 7.9 mm, respectively. Ideally, the parallel light should converge to a small point close to the diffraction limit. However, owing to the existence of spherical aberration, the spot size is larger than that in the ideal case. The focal plane region marked with a red circle, shown in Fig. 1(a), is amplified and displayed

Manuscript received April 13, 2017; revised August 23, 2017; accepted November 8, 2017. Date of publication November 13, 2017; date of current version February 22, 2018. This work was supported in part by the National Key Research and Development Program of China and in part by the National Natural Science Foundation of China under Grant 2017YFB1104601, Grant 61590930, Grant 2014CB921302, Grant 61435005, and Grant 51335008. *(Corresponding author: Qi-Dai Chen.)*

Z.-N. Tian, J.-G. Hua, F. Yu, Y.-H. Yu, and Q.-D. Chen are with the State Key Laboratory of Integrated Optoelectronics, College of Electronic Science and Engineering, Jilin University, Changchun 130012, China (e-mail: chenqd@jlu.edu.cn).

H. Liu is with the Center for Advanced Optoelectronic Functional Materials Research, Northeast Normal University, Changchun 130024, China, and also with the Key Laboratory for UV-Emitting Materials and Technology of Ministry of Education, Northeast Normal University, Changchun 130024, China.

H.-B. Sun is with the State Key Laboratory of Integrated Optoelectronics, College of Electronic Science and Engineering, Jilin University, Changchun 130012, China, also with the State Key Laboratory of Precision Measurement and Instruments, Department of Precision Instrument, Tsinghua University, Beijing 100084, China.

Color versions of one or more of the figures in this letter are available online at http://ieeexplore.ieee.org.

Digital Object Identifier 10.1109/LPT.2017.2772884

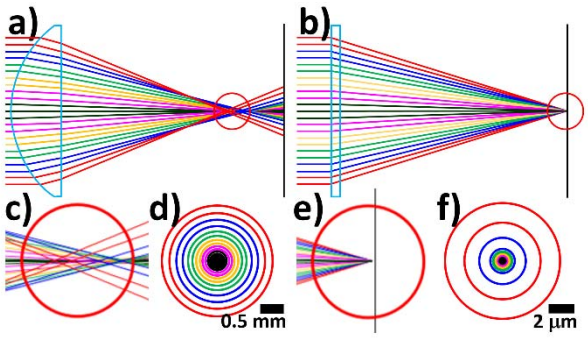

Fig. 1. Focusing simulated diagram of a spherical lens (a, c, d) and an aplanatic zone plate (b, e, f) based on the ray tracing method. (a) and (b): side view of the beam focusing with different apertures. (c) and (e): magnification images of the focal position in (a) and (b). (d) and (f): light spot on the focal plane.

in Fig. 1(c). It is clear that the light from different apertures is converging to different positions on the optical axis. The focus of the large aperture light, represented by the red line, is closer to the lens than that of the small aperture light, represented by the black line. On the focal plane, beams with different apertures converge into the light spot shown in Fig. 1(d). The root mean square (RMS) radius is about 193 μm, which is the smallest spot size that can be obtained on the optical axis. We designed a buried diffractive zone plate to reduce the spherical aberration of lens. The continuous phase change across the surface of the axis symmetric diffraction element can be expressed by the following formula:

$$\Phi = M \sum_{i=1}^{N} A_i \rho^{2i} \tag{1}$$

where A_i is the coefficient of radius ρ, which determines the phase distribution and optical properties of the diffractive element. The N is equal to 2 in the design, which means the phase distribution is described by a fourth-order polynomial. Through optical design software Zemax (Radiant Zemax), A_1 and A_2 are optimized to -243.808676 and 0.136186, respectively. Fig. 1(b) shows the focusing characteristics of the aplanatic zone plate, whose diameter and effective focal length are 10 mm and 20 mm, respectively. These values are equal to those of the spherical lens. The magnification of the focal position is shown in Fig. 1(e). It is obvious that the incident beams with different apertures converge to the same position on the optical axis. The RMS radius is about 1.48 μm [Fig. 1(f)], which is much smaller than that of the spherical lens [Fig. 1(d)].

The aplanatic zone plate was fabricated inside a z-cut sapphire crystal. Sapphire is an important optical material with many excellent optical properties, such as chemical stability, temperature resistance, wide transmittance spectrum, and high hardness. However, it is very difficult to machine with high precision using traditional processing methods. We used FsLDW technology to process the buried zone plate. By properly controlling the laser power, femtosecond laser can change the refractive index of a material without causing damage to it. We used a laser source (Light-Conversion Pharos) delivering less than 290-fs pulses of 1030-nm wavelength light at a repetition rate of 200 kHz. A 343-nm pulse generated by an integrated third harmonic generation system was used for improving machining accuracy. The femtosecond pulse was focused by a reflecting objective (Thorlabs LMM-40X-P01), whose magnification and numerical aperture are 40 and 0.5, respectively. The laser pulse energy was 2.2 μJ before the objective. The z-cut sapphire crystal wafer with a thickness of 500 μm was placed on the air-bearing rotary stage (Aerotech ABRT-150). For uniform exposure, the rotary stage was rotated at a constant linear speed of 5 mm per second.

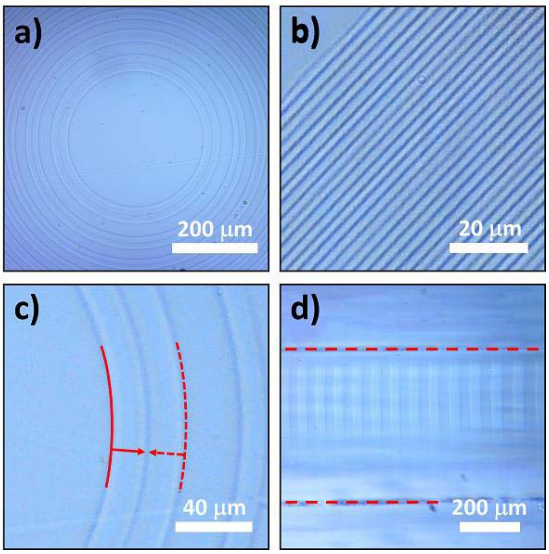

Fig. 2. Optical microscope images of the aplanatic zone plate, central region (a), marginal region (b), and cross section (d). (c) The inner-outer splicing method for accurately controlling the position and width of zones.

The optical microscope images of the zone plate are shown in Fig. 2. The significant difference between the scanned region and the un-scanned region can be observed clearly owing to the change of the refractive index caused by femtosecond laser irradiation. The central zone and the marginal zone are shown in Fig. 2(a) and Fig. 2(b), respectively. With the increase of radius, the phase function changes rapidly, which results in that both the zone width and the difference of zone widths to become very small. In order to process the zones accurately, the inner-outer splicing method was used, as shown in Fig. 2(c). The red line and the dashed line mark the inner and outer boundaries of the zone. The laser scanned from the inner boundary at 400 nm intervals outward the middle position, then jumped to the outer boundary, and scanned inward the middle position along the red dashed arrow. By this splicing scanning method, the boundaries and widths of zones can be controlled precisely. Fig. 2(d) shows the side view of the refractive index change induced by femtosecond pulse irradiation. This section of the sapphire wafer was polished, and the upper and lower surfaces were marked with red dashed lines. The area of the longitudinal refractive index change is greater than 200 μm.

III. Results and Discussion

The aplanatic characteristic of the zone plate has been tested and compared with a spherical lens and an aspherical lens (GoldDragon Optics Electronic Technology). The zone

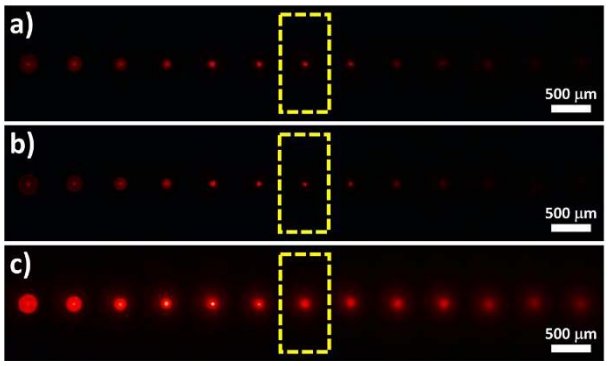

Fig. 3. Light spots behind aplanatic zone plate (a), aspherical lens (b), and spherical lens (c). Each spot image was taken at different positions on the optical axis. The distance between two adjacent spot images is 200 μm.

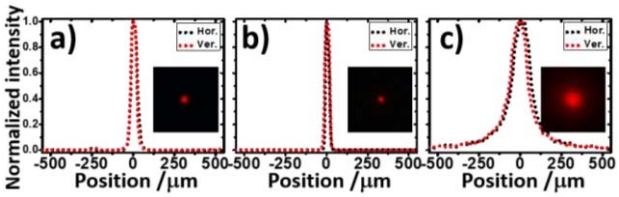

Fig. 4. The light spots of aplanatic zone plate (a), aspherical lens (b) and spherical lens (c). The insert images size are 500 μm.

plate and the lenses have the same diameter and focal length, which are 10 mm and 20 mm, respectively. A He-Ne laser with wavelength of 632.8 nm was used as a light source. We fixed the position of light source and the zone plate, and then measured the spot shape behind the zone plate with a charge-coupled device (CCD). By changing the positon of the CCD, the light spots at different positions were measured in turn. Fig. 3 shows the light spots behind the optical elements. Fig. 3(a), (b) and (c) show the focusing conditions of the zone plate, aspherical lens and spherical lens, respectively. The distance between two adjacent spot images is 200 μm. The minimum light spots are marked with a yellow dashed box. The light spots of zone plate and aspherical lens are obviously smaller than that of spherical lens. Moving detector from focus positions, the spots of zone plate and aspherical lens both enlarged obviously, which resulted from the simultaneous divergence of different aperture beams, as shown in Fig. 1(b). However, the light spots of spherical lens did not change obviously with the positions of detector. It is because the different aperture beams focus on the different positons on optical axis, as shown in Fig. 1(a).

For a more detailed analysis, the light spots on the focal plane are quantitatively characterized in Fig. 4. Fig. 4(a) and (b) show the spots size of zone plate and aspherical lens, which are significantly smaller than that of spherical lens shown in Fig. 4(c). The black and red curves represent the intensity distribution in the horizontal and vertical directions, respectively. The spot diameters of the zone plate and the aspherical lens in two directions are 40.6 μm, 43.3 μm and 27.1 μm, 28.2 μm, respectively. They are both smaller than 153.6 μm and 155.2 μm of the spherical lens. The smaller spot size benefits from all aperture beams were focusing on

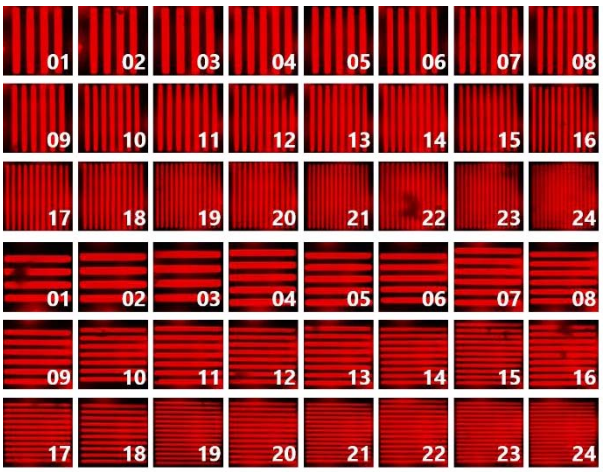

Fig. 5. Images of the zone plate with the resolution chart in the vertical and the horizontal directions. The line width ranges from 40 μm to 10 μm in the resolution chart. The length of each picture is 4 mm.

the optical axis simultaneously, which is the most direct and powerful proof of aplanatic characteristics.

Imaging is an important optical property for micro optical elements. Quantitative characterization is very necessary and urgent for evaluation and classification of micro optical components. Here, the imaging property of an aplanatic zone plate was quantitatively evaluated by using a resolution chart, which consists of different widths of bright and dark line pairs along the vertical and horizontal directions. The widths of the lines range from 10 μm to 40 μm with a length of 350 μm. The resolution chart was placed in front of the zone plate, which was illuminated by a light source with wavelength of 632.8 nm. The image was measured directly by a CCD positioned after the zone plate. Fig. 5 shows the imaging results of the zone plate with the resolution chart. The length of the line pairs in the images was 3.952 mm. Based on the relationship between the object and image, the distances from the zone plate to the resolution chart and the CCD can be calculated as 21.77 mm and 245.99 mm, respectively. Qualitatively, the images are clear without obvious differences. However, the contrast of the line pairs was reduced with the decreasing width.

The modulation transfer function (MTF) is recognized as a scientific optical evaluation standard, whose axes are the spatial frequency of line pairs and the contrast of their images in the horizontal and the vertical directions. The MTFs of experimental measurements and theoretical simulations are shown in Fig. 6. As the spatial frequency increases, the MTF with filed angle of 0 degree decreases slowly, while the MTFs with field angle of 2.5 and 5.0 degree drop quickly. It shows that the aplanatic zone plate has good properties in paraxial condition. In Fig. 6(a), the MTF of 0 degree filed was calculated from the images in Fig. 5. The images numbered 1, 5, 9, 12, 16, 20, and 24 were used, whose corresponding spatial frequencies are 12.5 line pairs per millimeter (lp/mm), 15.8 lp/mm, 19.8 lp/mm, 25.0 lp/mm, 31.4 lp/mm, 39.7 lp/mm, 50.0 lp/mm, respectively. At the spatial frequency of 50 lp/mm, the MTF was higher than 0.40 in both horizontal and vertical

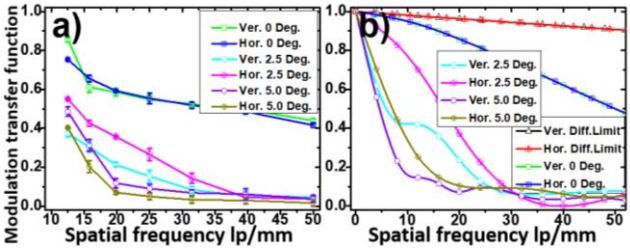

Fig. 6. Modulation transfer function of experimental measurements (a) and theoretical simulations (b).

directions. The aplanatic zone plate has a good imaging resolution, which is reflected by the precise control of the position and width of the diffractive zones.

IV. Conclusions

In summary, we succeeded in designing and fabricating a special aplanatic zone plate. The zone plate was embedded in a z-cut sapphire crystal by femtosecond laser direct writing technology. The performance of reducing spherical aberration was quantitatively characterized and compared with that of a spherical lens and an aspherical lens. This showed an obvious effect on the focal spot sizes and their positions. The imaging capability was quantitatively characterized by a resolution chart. The MTF was higher than 0.35 at 50 lp/mm. The work will open up a new mean of fabricating super-hard optical materials, and propose their applications in integrated and miniaturized optical systems, especially in complex and harsh environments. In addition, this work has significant meaning in quantitative characterization and evaluation of micro optical elements.

References

[1] M. Mizoshiri, H. Nishiyama, T. Kawahara, J. Nishii, and Y. Hirata, "SiO_2-based hybrid diffractive–refractive lenses fabricated by femtosecond laser-assisted micromachining," *Appl. Phys. Exp.*, vol. 1, no. 12, p. 127001, Dec. 2008.

[2] X. Meng *et al.*, "A simple way to fabricate close-packed high numerical aperture microlens arrays," *IEEE Photon. Technol. Lett.*, vol. 25, no. 14, pp. 1336–1339, Jul. 15, 2013.

[3] M. Malinauskas *et al.*, "Ultrafast laser processing of materials: From science to industry," *Light, Sci. Appl.*, vol. 5, p. e16133, Aug. 2016.

[4] S. Petsch, S. Schuhladen, L. Dreesen, and H. Zappe, "The engineered eyeball, a tunable imaging system using soft-matter micro-optics," *Light, Sci. Appl.*, vol. 5, p. e16068, Jul. 2016.

[5] Z. Deng *et al.*, "Dragonfly-eye-inspired artificial compound eyes with sophisticated imaging," *Adv. Funct. Mater.*, vol. 26, no. 12, pp. 1995–2001, Mar. 2016.

[6] E. Maguid, I. Yulevich, D. Veksler, V. Kleiner, M. L. Brongersma, and E. Hasman, "Photonic spin-controlled multifunctional shared-aperture antenna array," *Science*, vol. 352, pp. 1202–1206, Apr. 2016.

[7] P. Wang, N. Mohammad, and R. Menon, "Chromatic-aberration-corrected diffractive lenses for ultra-broadband focusing," *Sci. Rep.*, vol. 6, p. 21545, Feb. 2016.

[8] D. Wu, L. G. Niu, Q. D. Chen, R. Wang, and H. B. Sun, "High efficiency multilevel phase-type fractal zone plates," *Opt. Lett.*, vol. 33, no. 24, pp. 2913–2915, Dec. 2008.

[9] Q. Q. Zhang *et al.*, "A modified fractal zone plate with extended depth of focus in spectral domain optical coherence tomography," *J. Opt.*, vol. 13, p. 055310, May 2011.

[10] R. Bittner, "Tolerancing of single point diamond turned diffractive optical elements and optical surfaces," *J. Eur. Opt. Soc. Rapid Publ.*, vol. 2, p. 07028, Nov. 2007.

[11] J. Overbuschmann, J. Hengster, S. Irsen, and T. Wilhein, "Fabrication of Fresnel zone plates by ion-beam lithography and application as objective lenses in extreme ultraviolet microscopy at 13 nm wavelength," *Opt. Lett.*, vol. 37, no. 24, pp. 5100–5102, Dec. 2012.

[12] E. Di Fabrizio and M. Gentili, "X-ray multilevel zone plate fabrication by means of electron-beam lithography: Toward high-efficiency performances," *J. Vac. Sci. Technol. B, Microelectron. Process. Phenom.*, vol. 17, no. 6, pp. 3439–3443, Dec. 1999.

[13] G. Du *et al.*, "Direct fabrication of seamless roller molds with gapless and shaped-controlled concave microlens arrays," *Opt. Lett.*, vol. 37, no. 21, pp. 4404–4406, Nov. 2012.

[14] D. Wu *et al.*, "100% fill-factor aspheric microlens arrays (AMLA) with sub-20-nm precision," *IEEE Photon. Technol. Lett.*, vol. 21, no. 20, pp. 1535–1537, Oct. 15, 2009.

[15] T. Gissibl, S. Thiele, A. Herkommer, and H. Giessen, "Two-photon direct laser writing of ultracompact multi-lens objectives," *Nature Photon.*, vol. 10, no. 8, pp. 554–560, Aug. 2016.

[16] K. Sugioka and Y. Cheng, "Ultrafast lasers—Reliable tools for advanced materials processing," *Light, Sci. Appl.*, vol. 3, p. e149, Apr. 2014.

[17] H. Chen, X. Chen, Y. Xia, D. Liu, Y. Li, and Q. Gong, "Beam coupling in 2 × 2 waveguide arrays in fused silica fabricated by femtosecond laser pulses," *Opt. Exp.*, vol. 15, no. 9, pp. 5445–5450, Apr. 2007.

[18] Y. Ju *et al.*, "Direct fabrication of a microfluidic chip for electrophoresis analysis by water-assisted femtosecond laser writing in porous glass," *Chin. Opt. Lett.*, vol. 11, no. 7, p. 072201, Jul. 2013.

[19] A. Wang *et al.*, "Mask-free patterning of high-conductivity metal nanowires in open air by spatially modulated femtosecond laser pulses," *Adv. Mater.*, vol. 27, no. 40, pp. 6238–6243, Oct. 2015.

[20] L. Wang *et al.*, "Plasmonic nano-printing: Large-area nanoscale energy deposition for efficient surface texturing," *Light, Sci. Appl.*, vol. 6, p. e17112, Dec. 2017.

[21] A. Marcinkevičius *et al.*, "Femtosecond laser-assisted three-dimensional microfabrication in silica," *Opt. Lett.*, vol. 26, no. 5, pp. 277–279, Mar. 2001.

[22] Y. Li, Y. Dou, R. An, H. Yang, and Q. Gong, "Permanent computer-generated holograms embedded in silica glass by femtosecond laser pulses," *Opt. Exp.*, vol. 13, no. 7, pp. 2433–2438, Apr. 2005.

[23] S. Gross, M. J. Withford, and A. Fuerbach, "Direct femtosecond laser written waveguides in bulk Ti3+:sapphire," *Proc. SPIE*, vol. 7589, p. 75890U, Feb. 2010.

[24] Z.-N. Tian, J.-G. Hua, J. Hao, Y.-H. Yu, Q.-D. Chen, and H.-B. Sun, "Micro-buried spiral zone plate in a lithium niobate crystal," *Appl. Phys. Lett.*, vol. 110, no. 4, p. 041102, Jan. 2017.